Hyperfine contribution to spin-exchange frequency shifts in the hydrogen maser

B. J. Verhaar, J. M. V. A. Koelman, H. T. C. Stoof, and O. J. Luiten
Department of Physics, Eindhoven University of Technology, 5600 MB Eindhoven, The Netherlands

S. B. Crampton
Department of Physics and Astronomy, Williams College, Williamstown, Massachusetts 01267
(Received 18 December 1986)

We have rigorously included hyperfine interactions during electron-spin-exchange collisions between ground-state hydrogen atoms and find additional frequency shifts which are significant for low-temperature atomic hydrogen maser oscillators.

I. INTRODUCTION

Electron-spin-exchange collisions between ground-state paramagnetic atoms are usually treated in a degenerate-internal-states approximation, which ignores hyperfine interactions relative to electron-exchange interactions during collisions.[1–5] Such calculations predict small shifts of the $\Delta m_F=0$ hyperfine transition frequency in ground-state atomic hydrogen proportional to the rate of collisions with other hydrogen atoms and to the difference between the two $\Delta m_F=0$ level populations.[4,5] Because of the proportionality to the level population difference, such shifts can be eliminated from the frequency of an atomic hydrogen maser oscillating in weak magnetic field on the $\Delta m_F=0$ transition by tuning the maser microwave cavity so that there is no change of oscillation frequency with collision rate.[6] A semiclassical treatment by one of us of hyperfine effects during collisions to first order revealed a small additional shift of the $\Delta m_F=0$ hydrogen maser oscillation frequency not compensated for by cavity mistuning.[7] Both the degenerate-internal-states shift and the additional hyperfine-induced shift have been confirmed near room temperature,[7,8] and the degenerate-internal-states shift down to liquid-nitrogen temperatures.[9]

Recently, hydrogen maser oscillation has been achieved at 9 to 10.5 K using solid-neon storage surfaces,[10,11] and at 0.3 to 0.6 K using superfluid-helium storage surfaces.[12–14] For cryogenic masers operating with reduced thermal noise and potentially greater radiated power, the instability due to thermal noise may be[15–17] as low as two parts in 10^{18}. The actual instability minimum will be determined by mechanisms which couple the maser frequency to instabilities of other maser parameters. Understanding the magnitudes and level population dependences of any uncompensated hyperfine-induced spin-exchange-collision frequency shifts is therefore potentially important to using cryogenic hydrogen masers as frequency standards and spectroscopic tools. At cryogenic temperatures the effects of atom identity and quantization of collision angular momenta are significant, so that it is essential that calculations be fully quantum mechanical. Berlinsky and Shizgal have extended the quantum-mechanical degenerate-internal-states calculations to 10 K and below.[18] We report here a quantum-mechanical treatment of frequency shifts and broadening due to H-H spin-exchange collisions at low temperatures, including hyperfine-induced effects. We find effects which are large compared to the potential thermal instabilities of cryogenic hydrogen masers, but may also provide a sensitive probe of nonadiabatic contributions in hydrogen-hydrogen atom-atom interactions at low collision energies.

II. METHOD

Our starting point is the evolution equation for the spin density matrix,

$$\frac{d\rho_{\kappa\kappa'}}{dt}=-\frac{i}{\hbar}(E_\kappa-E_{\kappa'})\rho_{\kappa\kappa'}-\frac{i}{\hbar}[H_1(t),\rho]_{\kappa\kappa'}$$
$$+n_{\mathrm{H}}\sum_{\lambda,\mu,\nu,\mu',\nu'}\sum_{l,m,l',m'}\rho_{\mu\mu'}\rho_{\nu\nu'}[(1+\delta_{\kappa\lambda})(1+\delta_{\kappa'\lambda})(1+\delta_{\mu\nu})(1+\delta_{\mu'\nu'})]^{1/2}$$
$$\times\left\langle\frac{\pi\hbar}{m_{\mathrm{H}}k}(S_{\{\kappa\lambda\}lm,\{\mu\nu\}l'm'}S^*_{\{\kappa'\lambda\}lm,\{\mu'\nu'\}l'm'}-\delta_{\{\kappa\lambda\},\{\mu\nu\}}\delta_{\{\kappa'\lambda\},\{\mu'\nu'\}}\delta_{ll'}\delta_{mm'})\right\rangle+\left.\frac{d\rho_{\kappa\kappa'}}{dt}\right|_{\mathrm{rel}},\qquad(1)$$

the quantum-mechanical Boltzmann equation for a homogeneous system, which we have derived from the fundamental Bogoliubov-Born-Green-Kirkwood-Yvon (BBGKY) hierarchy for the distribution matrices. In this equation Greek subscripts take values a,b,c,d, the $1s$ hyperfine states in order of increasing energy E_α (Fig. 1). The operator $H_1(t)$ represents any (time-dependent but position-independent) magnetic field operating on the atoms. The last term represents all relaxation terms except for the relaxation due to the two-body collisions tak-

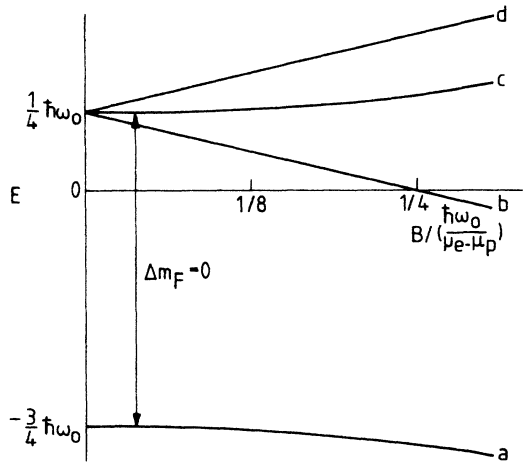

FIG. 1. Atomic hydrogen ground-state energy levels vs applied magnetic field strength in units $(\hbar\omega_0)/(\mu_e-\mu_p)$ (=0.102 T).

en into account in the previous term. The hydrogen density is denoted by n_H, the atomic mass by m_H, and the wave number in the entrance channels of the S-matrix elements by k. The notation $\{\alpha\beta\}$ implies normalized symmetrization (antisymmetrization) of two-body spin states for relative orbital angular momentum l even (odd) having z component m. The brackets $\langle\ \rangle$ denote thermal averaging with the same velocity distribution for each of the spin states, assuming dominance of thermalizing elastic collisions with the walls or between atoms relative to inelastic collisions between atoms.

Considering situations with coherence only between the a and c levels, we have a 4×4 spin density matrix with only one pair of nonvanishing off-diagonal elements $\rho_{ac}=\rho_{ca}^*$. The collision terms in Eq. (1) contributing to the time development of ρ_{ac} have the form

$$\left.\frac{d\rho_{ac}}{dt}\right|_{\text{coll}}=n_H\rho_{ac}\sum_\nu \tilde{G}_\nu\rho_{\nu\nu} \tag{2}$$

with rate-constant-like[19] coefficients $\tilde{G}_\nu$.

Let us now look more closely at the nature of these coefficients on the basis of some symmetry considerations. The S-matrix elements follow from the Schrödinger equation for two-body scattering. This contains a central interaction V^c consisting of singlet and triplet potentials,

$$V^c=P_S V_S(r)+P_T V_T(r)\ , \tag{3}$$

P_S (P_T) standing for a projection on singlet (triplet) subspaces. In addition, it contains the intraatomic hyperfine interactions,

$$V^{\text{hf}}=\hbar\omega_0(\mathbf{S}_1\cdot\mathbf{I}_1+\mathbf{S}_2\cdot\mathbf{I}_2) \tag{4}$$

in which ω_0 is the hyperfine frequency, while $\mathbf{S}_{1,2}$ and $\mathbf{I}_{1,2}$ are the electron and proton spins of the two colliding atoms. We consider only the case of very weak external magnetic fields and so leave out Zeeman terms in calculating the S-matrix elements. Although these terms, the interatomic hyperfine interactions, and the spin dipolar interactions can be included in our coupled-channel calculations,[20] their effects are negligible compared to the exchange and intraatomic hyperfine interactions. We leave them out both in the discussion of symmetries and in the later first-order treatment so as to keep the physics as transparent as possible.

Each of the coefficients $\tilde{G}_\nu$ then contains a sum of products $S_{\{a\alpha\}l,\{a\nu\}l}S^*_{\{c\alpha\}l,\{c\nu\}l}$, independent of m. It turns out that only elastic S-matrix elements contribute. For odd l this follows from the selection rule $\Delta m_F=0$, taking into account that antisymmetric spin states $\{a\nu\}$ and $\{c\nu\}$ can be formed simultaneously only for $\nu=b$ or d. For even l it is due to assuming zero magnetic field: All five symmetric spin states consisting of two different hyperfine states, at least one of which is a or c, have unmixed $S=1$, so that no coupling by V^c (or V^{hf}) occurs within this set or to aa and cc. The five $S=1$ spin states having elastic S-matrix elements $\exp(2i\delta_{lT})$, with δ_{lT} the triplet phase shift, the S-matrix products within $\tilde{G}_\nu$ are cancelled by the corresponding products of Kronecker deltas for $\nu=b$ or d. Therefore, in Eq. (2) the $\nu=b$ and d terms have contributions from odd l only, the $\nu=a$ and c terms from even l only.

The collision problem shows symmetry under a 180° combined rotation of the two electron spins and two proton spins about an axis perpendicular to the weak magnetic field. This rotation exchanges b and d while leaving a and c alone. We conclude that the S-matrix elements for the ab and ad spin states are equal, as are those for the spin states cb and cd. The result is finally that $\tilde{G}_\nu=\langle v\lambda_\nu\rangle=\langle v\rangle\bar{\lambda}_\nu$ with $\langle v\rangle$ the thermal average collision speed and $\bar{\lambda}_\nu$ the thermal average of the λ_ν "cross section" defined in simplified notation as

$$\begin{aligned}
\lambda_a&=\frac{2\pi}{k^2}\sum_{l\ even}(2l+1)[S^l_{aa}(S^l_{\{ac\}})^*-1]\ ,\\
\lambda_c&=\frac{2\pi}{k^2}\sum_{l\ even}(2l+1)[S^l_{\{ac\}}(S^l_{cc})^*-1]\ ,\\
\lambda_b&=\lambda_d=\frac{\pi}{k^2}\sum_{l\ odd}(2l+1)[S^l_{\{a\nu\}}(S^l_{\{c\nu\}})^*-1]\ ,\qquad \nu=b\text{ or }d\ .
\end{aligned} \tag{5}$$

We stress that all of the S-matrix elements in Eq. (5) are to be calculated for a common value of kinetic energy in the particular elastic channel.

Substituting

$$\rho_{ac}(t)=\rho_{ac}(0)\exp[i(\omega_0+\delta\omega+i\tau_2^{-1})t]$$

and using $\sum_\nu\rho_{\nu\nu}=1$, we find for the frequency shift

$$\delta\omega=n_H\langle v\rangle[(\rho_{cc}-\rho_{aa})\bar{\lambda}_0+(\rho_{cc}+\rho_{aa})\bar{\lambda}_1+\bar{\lambda}_2] \tag{6}$$

in which

$$\begin{aligned}
\lambda_0&=\text{Im}[(\lambda_c-\lambda_a)/2]\ ,\\
\lambda_1&=\text{Im}[(\lambda_c+\lambda_a)/2-\lambda_b]\ ,\\
\lambda_2&=\text{Im}(\lambda_b)\ .
\end{aligned} \tag{7}$$

At this point it is interesting to indicate how these results reduce to those of Balling *et al.* when the hyperfine splitting is turned off. The channels can then be decou-

pled by transforming to the triplet and singlet channels, leading to the expressions

$$S^{l(0)}_{\{\alpha\beta\}} = \langle \{\alpha\beta\} \mid e^{2i\delta_{lS}} P_S + e^{2i\delta_{lT}} P_T \mid \{\alpha\beta\} \rangle \tag{8}$$

for the S-matrix elements in the degenerate-internal-states approximation as expectation values in (anti)symmetric spin states depending on l. Alternatively, we may note that without $V^{\rm hf}$ the Hamiltonian for the two-body problem no longer depends on the proton- spin degrees of freedom. A combined rotation of proton spins by 180° about the magnetic field direction as an additional symmetry operation now exchanges a and c while leaving b and d alone. We then find

$$\lambda_0^{(0)} = \frac{\pi}{2k^2} \sum_{l \text{ even}} (2l+1) \sin[2(\delta_{lT} - \delta_{lS})] ,$$

$$\lambda_1^{(0)} = \lambda_2^{(0)} = 0 . \tag{9}$$

The frequency shift $\delta\omega$ thus reduces to the well-known expression for the case of vanishing hyperfine splitting ($\lambda_0^{(0)} = -\frac{1}{4}\lambda^+$ of Ref. 18).

To determine the various λ quantities without neglecting hyperfine splitting, we have to calculate the elastic S-matrix elements in Eq. (5). This can be done by integrating the coupled radial equations describing the H-H scattering wave functions in the various channels: the so-called coupled-channels (CC) approach,[20,21] which in principle yields exact results. This is one of the methods we have used.

Calculating the frequency shift by the CC approach over the wide temperature interval needed for thermal averaging would be rather time consuming. Instead, it is attractive to use an approach which exploits the weakness of the hyperfine interaction ($\hbar\omega_0 \approx 0.068$ K) in the form of a calculation that takes into account the hyperfine interaction as a first-order correction to the degenerate-internal-states approximation. However, a simple Born-type approach for the hyperfine interaction yields volume integrals which do not converge. This difficulty stems from the fact that the hyperfine interaction does not fall off at large distances. Yet as pointed out in Ref. 22, a first-order treatment is possible and leads to a Born-type integral restricted to a finite volume beyond which the singlet and triplet potentials are negligible, accompanied by a Wronskian surface term which in a way accounts for the nonvanishing hyperfine interaction in the outer volume. We use this method to calculate the various elastic S-matrix elements including the finite energy separation of other hyperfine energy levels from the hyperfine energy level associated with the particular elastic channel under consideration. The first-order corrections then arise from back and forth transitions to other hyperfine levels during a collision, as in the semiclassical treatment.[7] We find that the corrections to the degenerate-internal-states S-matrix elements are given by

$$\Delta S^l_{\{\alpha\beta\}} = \langle \{\alpha\beta\} \mid (P_T - P_S)(V^{\rm hf} - E_\alpha - E_\beta)(P_T - P_S) \mid \{\alpha\beta\} \rangle \Delta^l , \tag{10}$$

i.e., a simple spin matrix element times a quantity Δ^l given by

$$\Delta^l = \frac{i}{4} \frac{m_{\rm H}}{\hbar^2 k^2} \left[k \int_0^{r_0} [u_S^{l(0)}(k,r) - u_T^{l(0)}(k,r)]^2 dr + \tfrac{1}{2}(S_S^{l(0)} - S_T^{l(0)})^2 W \left[O^l(kr), \frac{\partial}{\partial k} O^l(kr) \right]_{r=r_0} \right] , \tag{11}$$

with the Wronskian W defined as $W[f,g] = f\,\partial g/\partial r - \partial f/\partial r\, g$. The radial wave functions $u^{l(0)}$ are normalized so as to have asymptotic behavior

$$e^{-i(kr - l\pi/2)} - S^{l(0)} e^{i(kr - l\pi/2)} ,$$

and $O^l(kr)$ is a Hankel-like free outgoing wave with asymptotic behavior $e^{i(kr - l\pi/2)}$. Expression (11) is independent of r_0 under the condition that the triplet and singlet potentials are zero for $r > r_0$.

Substituting the S-matrix elements including the first-order corrections into (5), we find for the right-hand side of (7):

$$\begin{aligned} \lambda_0 &= \lambda_0^{(0)} - \tfrac{1}{2}\Delta\lambda_+ , \\ \lambda_1 &= \Delta\lambda_+ - \Delta\lambda_- , \\ \lambda_2 &= \Delta\lambda_- , \end{aligned} \tag{12}$$

with the corrections to the degenerate-internal-states $\lambda_i^{(0)}$ values of Eq. (9) given by

$$\begin{aligned} \Delta\lambda_+ &= \frac{\pi}{2k^2} \sum_{l \text{ even}} (2l+1) \operatorname{Im}(2\Delta^{l*} S_T^{l(0)}) , \\ \Delta\lambda_- &= \frac{\pi}{2k^2} \sum_{l \text{ odd}} (2l+1) \operatorname{Im}[\Delta^{l*}(S_T^{l(0)} + S_S^{l(0)})] . \end{aligned} \tag{13}$$

Equations (6), (7), and (5) represent our final formulation of the spin-exchange frequency shift including the hyperfine contributions. In Sec. III these equations form the basis of a coupled-channel calculation. Likewise, Eqs. (12), (13), and (11) are used for a first-order calculation.

III. RESULTS

Both in the CC calculation and in the first-order approximation we have used "state-of-the-art" singlet and triplet potentials.[23,24] Details of the CC calculation are given in Refs. 20 and 21. With respect to nonadiabatic effects, two types of calculations have been carried out. The first incorporates the departure from the Born-Oppenheimer approximation together with relativistic and radiative effects only as first-order corrections to the singlet and triplet potentials, as in Ref. 24, Sec. III. This approach is commonly called the "adiabatic" approximation. Wolniewicz (Ref. 24, Sec. IV) has devised a method for including the departure from Born-Oppenheimer in the bound-state energies to second order (usually referred to as "nonadiabatic" corrections), but this method does not apply to the continuum. Our own calculations and those of Ref. 25 indicate that the second-order corrections

to the bound-state energies nearest the continuum can be reproduced by simply replacing the reduced proton mass $m_p/2$ by the reduced atomic mass $m_H/2$ in the first-order calculation. In the second type of calculation we incorporate nonadiabatic effects into the continuum calculation by replacing the reduced mass $\mu=m_p/2$ by $\mu=m_H/2$ in the radial Schrödinger equation. Results show a remarkable sensitivity to this introduction of nonadiabaticity, far greater than would be expected from the relative change of the reduced-mass parameter μ from $m_p/2$ to $m_H/2$. In view of the large collection of results involved, we restrict the following figures to results calculated using $\mu=m_H/2$. In discussing these figures, the most important differences with the adiabatic results will be indicated.

In Fig. 2 we give the contributions of the partial waves $l=0,1,2,3$ to λ_1, and of the partial waves $l=1,3$ to λ_2, as functions of energy. The hyperfine-induced correction to λ_0 is small and does not seem to be significant. Note that the low-energy behavior in Fig. 2 is proportional to $E^{l-1/2}$, in accordance with expectations. This figure makes clear that the first-order treatment is indeed of considerable help in covering the large energy range and the large number of partial waves needed to calculate Boltzmann-averaged values over the temperature range of interest: Comparing the CC results with the first-order results, the first-order calculation gives very accurate results except at low energies in the $l=0$ partial wave. The deviation takes the form of a prominent cusp in the CC curve due to the threshold of the *cc* channel felt in the *aa* channel at $E=2\hbar\omega_0$. This threshold behavior is easily understood by noting that each of the S-matrix elements involved is a regular analytic function[26] of the channel opening up at the threshold. Purely imaginary values for this wave number below threshold, changing into real values above, explain the calculated result that the path which is followed by $S_{aa}^{l=0}$ in the complex plane shows a 90° kink. The latter gives rise to the cusp behavior in Fig. 2. It is understandable that it cannot be reproduced by a first-order treatment based on the idea that the hyperfine interaction has a small effect. However, it is clear that the hyperfine separation of the *aa* and *cc* thresholds is of primary importance at low energies. In a classical picture the hyperfine precession angle of spins during a collision is no longer small for collisions with a longer duration at threshold.

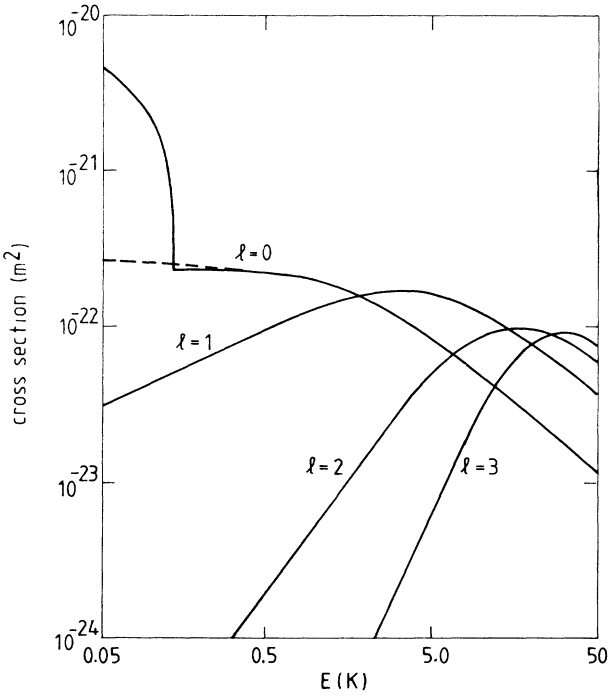

FIG. 2. Partial contributions of the first four partial waves to the hyperfine-induced frequency shift cross sections as functions of energy: $-\lambda_1^l$ for even l and $\lambda_1^l=-\lambda_2^l$ for odd l. Solid lines, CC calculation; dotted line, first-order calculation where it differs significantly from the CC calculation.

From the same argument one might expect similarly large differences of CC and first-order results close to resonances, and that turns out to be the case. Calculations using reduced mass $\mu=m_P/2$ show a pronounced resonance behavior of the λ quantities in the $l=4$ partial wave due to the 14,4 vibration-rotation state in the continuum at 1.3 K. Close to resonance, the first-order treatment greatly overestimates the λ quantities, and Boltzmann averaging then leads to appreciable contributions by the resonance. The CC calculation shows two much-weaker resonances with a $2\hbar\omega_0$ hyperfine separation, corresponding to the energies at which the *aa* and *cc* channels are resonant. Boltzmann averaging these leads to a much smaller contribution by the resonance. Using $\mu=m_H/2$, the $v=14,j=4$ resonance shifts to lower energies in the continuum or even below the *aa* threshold,[27] depending on the radial extent of the 0.2-cm^{-1} "nonconvergence" correction of Ref. 24. In both cases the influence of the resonance is negligible.

Our earlier discussion of the $l=0$ partial wave dealt only with the difference between the CC and first-order results. The $l=0$ curve shows a remarkable sensitivity to μ. Replacing $\mu=m_H/2$ by the very nearly equal value $m_P/2$ leads to changes of up to 50% in Fig. 2. Even after Boltzmann averaging this difference is expected to be observable.

Figure 3 shows the temperature dependence of the thermally averaged quantities $\bar{\lambda}_1$ and $\bar{\lambda}_2$. For completeness we have also added $\bar{\lambda}_0$, $\bar{\sigma}_1=(\bar{\sigma}_+-\bar{\sigma}_-)/2$, and $\bar{\sigma}_2=\bar{\sigma}_-/2$, with $\bar{\sigma}_+$ ($\bar{\sigma}_-$) the thermal average spin-exchange broadening cross section[18,28] for even (odd) l. Our values for $\bar{\sigma}_1$, $\bar{\sigma}_2$, and $\bar{\lambda}_0$ differ significantly from those of Refs. 18 and 28. This is not due to hyperfine-induced contributions, which are negligible, but to differences in the potentials used to calculate them. Note that the high CC values of λ_1 below the cusp result in significant deviations of the first-order values close to the important temperature 0.5 K.

IV. SIGNIFICANCE FOR HYDROGEN MASERS

Although $\bar{\lambda}_1$ and $\bar{\lambda}_2$ are several orders of magnitude less than $\bar{\lambda}_0$ at the temperatures of interest to cryogenic hydrogen masers, they are significant because of the different

combinations of level populations ρ_{vv} that accompany their contributions to $\Delta m_F=0$ transition frequency shifts. Under conditions of self-excited maser oscillation, $\rho_{cc}-\rho_{aa}$ is fixed by the requirement that the power radiated by the atoms be equal to that dissipated in the microwave cavity and other electronics. Assuming a single Lorentzian microwave cavity mode and using the methods of Ref. 6 we find

$$\rho_{cc}-\rho_{aa}=\frac{\hbar V_c(1+\Delta^2)}{\mu_0\mu_B^2\eta Q V_b n_H \tau_2} \tag{14}$$

with $\Delta=Q(\omega_c/\omega-\omega/\omega_c)$ twice the ratio of cavity mistuning to cavity resonance width, μ_B the Bohr magneton, $\eta Vb/V_c$ a filling factor relating the rf energy density to the amplitude of rf field driving the $\Delta m_F=0$ transition,[29] and $1/\pi\tau_2$ the full frequency width (in Hz) of the $\Delta m_F=0$ transition. Substituting (14) into (6) and including the direct frequency pulling due to cavity mistuning,

$$\delta\omega=[\Delta+\alpha\bar{\lambda}_0(1+\Delta^2)]/\tau_2 + n_H\langle v\rangle[\bar{\lambda}_1(\rho_{cc}+\rho_{aa})+\bar{\lambda}_2] , \tag{15}$$

with $\alpha=(\langle v\rangle/\mu_0)(\hbar/\mu_B^2)(V_c/\eta Q V_b)$. The largest potential instability is due to cavity mistuning. Assuming linewidth $1/\pi\tau_2$ of order 1 Hz, cavity instabilities of parts in 10^5 of the cavity width would produce frequency instabilities of the order of parts in 10^{14} of the oscillation frequency, large compared to the 10^{-15} instabilities of room-temperature hydrogen maser standards[17] and very large compared to the potential thermal instabilities of cryogenic masers. In practice the cavity tuning must be reset by monitoring it either electronically, using external sources and detectors, or using variations of the oscillation frequency itself as some maser parameters are varied. Assuming linear dependence of the oscillation frequency on $1/\tau_2$, values of oscillation frequency measured for different values of $1/\tau_2$ and different values of Δ for $\Delta \ll 1$ can be used to correct the oscillation frequency to its "tuned" value: the value it would have if the cavity were tuned to produce no variation of oscillation frequency with $1/\tau_2$. Such methods[30] of setting the maser cavity are relatively insensitive to instabilities of coupling to external microwave sources and detectors. Moreover, in the absence of the frequency shifts proportional to $\bar{\lambda}_1$ and $\bar{\lambda}_2$, the tuned oscillation frequency would be unshifted by either cavity mistuning or collision effects. Because of the hyperfine-induced collision effects, such tuning methods may leave significant frequency offsets which can convert linewidth instabilities to instabilities of the tuned maser oscillation frequency.

To illustrate these effects we make use of

$$1/\tau_2=1/\tau_0+n_H\langle v\rangle[\bar{\sigma}_1(\rho_{cc}+\rho_{aa})+\bar{\sigma}_2] , \tag{16}$$

the second term of which is obtained by a derivation[5] similar to that of (6), but ignoring hyperfine-induced effects which are negligible. Here $1/\tau_0$ includes all contributions to the linewidth not due to gas-phase spin-exchange collisions. Surface spin-exchange and recombination effects are small because the surface gas density

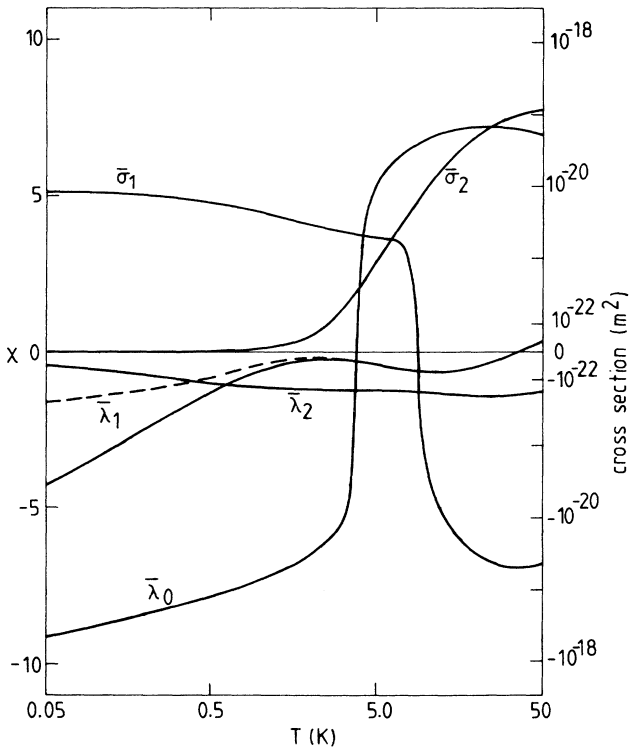

FIG. 3. Thermally averaged values of the various frequency shift and broadening cross sections as functions of temperature. To combine the advantages of a logarithmic plot for larger values of the cross sections and a linear plot for small values, the vertical scale is taken to be linear in $x=\text{arcsinh}(\bar{\sigma}_i/10^{-22}\ \text{m}^2)$ and $x=\text{arcsinh}(\bar{\lambda}_i/10^{-22}\ \text{m}^2)$, respectively. The horizontal scale is logarithmic. Solid lines, CC calculation; dotted line, first-order calculation where it differs significantly from the CC calculation.

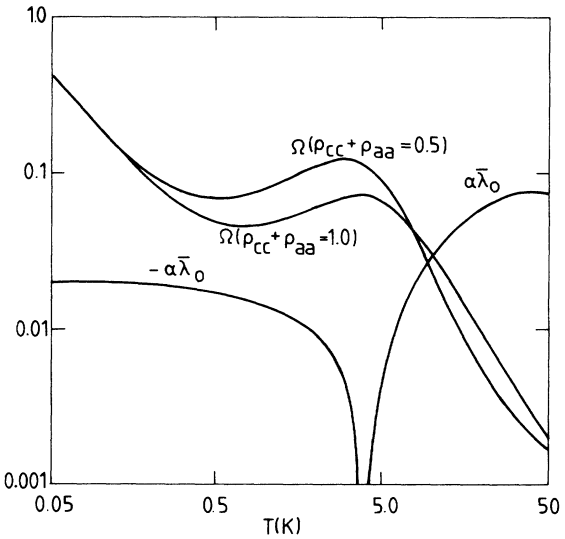

FIG. 4. The dimensionless frequency offset parameters $\alpha\bar{\lambda}_0$ and Ω as functions of temperature. Ω is given for $\rho_{cc}+\rho_{aa}$ (total fraction of atoms in a or c states) equal to 0.5 and 1.0, and $\bar{\alpha}\bar{\lambda}_0$ is given for $\eta Q V_b/V_c=1000$.

is very low under cryogenic maser operating conditions, so that $1/\tau_0$ is dominated by the rate at which atoms flow in and out of the maser storage volume, plus any relaxation by motion through magnetic field gradients. Using (16) to eliminate $n_H\langle v\rangle$ from (15), we find

$$\delta\omega=[\Delta+\alpha\bar{\lambda}_0(1+\Delta^2)-\Omega]/\tau_2+\Omega/\tau_0 \tag{17}$$

with

$$\Omega=-\frac{\bar{\lambda}_1(\rho_{cc}+\rho_{aa})+\bar{\lambda}_2}{\bar{\sigma}_1(\rho_{cc}+\rho_{aa})+\bar{\sigma}_2}\ . \tag{18}$$

Ω generally depends on $1/\tau_2$ in a complicated way via a $1/\tau_2$ dependence of $\rho_{cc}+\rho_{aa}$. However, there are several important cases when the $1/\tau_2$ dependence of Ω can be neglected. At very low temperatures $\bar{\lambda}_2\ll\bar{\lambda}_1$ and $\bar{\sigma}_2\ll\bar{\sigma}_1$, yielding $\Omega=-\bar{\lambda}_1/\bar{\sigma}_1$ independent of $\rho_{cc}+\rho_{aa}$. If any single relaxation rate greatly exceeds all others, $\rho_{cc}+\rho_{aa}$ and Ω are approximately constant as relaxation processes vary. To get an impression of the likely instabilities of maser oscillation frequency due to hyperfine-induced collision effects, we therefore neglect the $1/\tau_2$ dependence of Ω. In this approximation $\delta\omega$ varies linearly with $1/\tau_2$ as the density is varied. Correcting the oscillation frequency to the value it would have with the cavity tuned for no variation of oscillation frequency as the density is varied then leaves the tuned oscillation frequency offset by the last term in (17). Figure 4 gives Ω as a function of temperature for the choices $\rho_{cc}+\rho_{aa}=0.5$ and 1.0. We include values of $\alpha\bar{\lambda}_0$ calculated assuming $(\eta QV_b/V_c)=1000$, a value intermediate between its value in the first cryogenic masers[10–13] and its likely value in actual cryogenic maser standards. The very large increase of Ω relative to $\alpha\bar{\lambda}_0$ as the temperature is lowered illustrates the much greater importance of hyperfine-induced frequency shifts at cryogenic temperatures—for example, at 0.5 K and $\rho_{cc}+\rho_{aa}=0.5$, $\Omega=0.07$. Even this small value puts severe limits on maser parameter stabilities required to achieve maser frequency instability as low as 2 parts in 10^{18}. For $\Omega=0.07$ the maximum allowed instability of τ_0^{-1} would be $3\times10^{-7}\ s^{-1}$.

Note that measurements of changes of residual offset frequency with changes of τ_0^{-1} could be used both to reduce the hyperfine-induced frequency offsets and to measure $\bar{\lambda}_{1,2}$, as in the high-temperature investigations of hyperfine-induced spin-exchange frequency shifts.[7] Considering the sensitivity of the low-temperature spin-exchange cross sections $\bar{\sigma}_{1,2}$ and $\bar{\lambda}_{0,1,2}$ to details of the H-H interaction, in particular to nonadiabatic effects, such experiments may yield interesting results.

ACKNOWLEDGMENT

We acknowledge support from the Stichting voor Fundamenteel Onderzoek der Materie and National Science Foundation Grant No. PHY-8406467.

[1]E. M. Purcell and G. B. Field, Astrophys. J. **124**, 542 (1956).
[2]J. P. Wittke and R. H. Dicke, Phys. Rev. **103**, 620 (1956).
[3]A. Dalgarno, Proc. R. Soc. London, Ser. A **262**, 132 (1961).
[4]P. L. Bender, Phys. Rev. **132**, 2154 (1963).
[5]L. C. Balling, R. J. Hanson, and F. M. Pipkin, Phys. Rev. **133**, A607 (1964); **135**, AB1 (1964).
[6]S. B. Crampton, Phys. Rev. **158**, 57 (1967).
[7]S. B. Crampton and H. T. M. Wang, Phys. Rev. A **12**, 1305 (1975).
[8]S. B. Crampton, J. A. Duvivier, G. S. Read, and E. R. Williams, Phys. Rev. A **5**, 1752 (1972).
[9]M. Desaintfuscien, J. Viennet, and C. Audoin, J. Phys. (Paris) Lett. **36**, L-281 (1975).
[10]S. B. Crampton, Ann. Phys. (Paris) **10**, 893 (1985).
[11]S. B. Crampton, K. M. Jones, G. Nunes, and S. P. Souza, Proceedings of the Sixteenth Annual Precise Time and Time Interval (PTTI) Applications and Planning Meeting, Greenbelt, Maryland, 1985 [NASA Technical Memorandum No. 8756, 1985 (unpublished)], p. 339.
[12]H. F. Hess, G. P. Kochanski, J. M. Doyle, T. J. Greytak, and D. Kleppner, Phys. Rev. A **34**, 1602 (1986).
[13]M. D. Hürlimann, W. N. Hardy, A. J. Berlinsky, and R. W. Cline, Phys. Rev. A **34**, 1605 (1986).
[14]R. L. Walsworth, I. F. Silvera, H. P. Godfried, C. C. Agosta, R. F. C. Vessot, and E. M. Mattison, Phys. Rev. A **34**, 2550 (1986).
[15]W. D. Hardy and M. Morrow, J. Phys. (Paris) Colloq. **42**, C8-171 (1981).
[16]A. J. Berlinsky and W. D. Hardy, Proceedings of the Thirteenth Annual Precise Time and Time Interval (PTTI) Applications and Planning Meeting, Naval Research Laboratory, Washington, D. C. 1982 [NASA Conference Publication No. 2220, 1982 (unpublished)], p. 547.
[17]R. F. C. Vessot, M. W. Levine, and E. M. Mattison, Proceedings of the Ninth Annual Precise Time and Time Interval (PTTI) Applications and Planning Meeting, Greenbelt, Maryland, 1977 [NASA Technical Memorandum No. 78104, 1978 (unpublished)], p. 549.
[18]A. J. Berlinsky and B. Shizgal, Can. J. Phys. **58**, 881 (1977).
[19]A. Lagendijk, I. F. Silvera, and B. J. Verhaar, Phys. Rev. B **33**, 626 (1986).
[20]R. M. C. Ahn, J. P. H. W. van den Eijnde, and B. J. Verhaar, Phys. Rev. B **27**, 5424 (1983).
[21]J. P. H. W. van den Eijnde, Ph.D. thesis, Eindhoven University of Technology, The Netherlands, 1984.
[22]A. M. Schulte and B. J. Verhaar, Nucl. Phys. **A232**, 215 (1974).
[23]W. Kolos and L. Wolniewicz, J. Chem. Phys. **43**, 2429 (1965); W. Kolos and L. Wolniewicz, Chem. Phys. Lett. **24**, 457 (1974); J. F. Bukta and W. J. Meath, Mol. Phys. **27**, 1235 (1974).
[24]L. Wolniewicz, J. Chem. Phys. **78**, 6173 (1983).
[25]P. R. Bunker, C. J. McLarnon, and R. E. Moss, Mol. Phys. **33**, 425 (1977).
[26]L. Fonda, in *Fundamentals of Nuclear Theory*, edited by A. de-Salit and C. Villi (International Atomic Energy Agency,

Vienna, 1967), p. 351.
[27]M. W. Reynolds, I. Shinkoda, R. W. Cline, and W. N. Hardy, Phys. Rev. B **34**, 4912 (1986).
[28]A. C. Allison, Phys. Rev. A **5**, 2695 (1972); A. C. Allison and F. J. Smith, At. Data **3**, 317 (1971).
[29]D. Kleppner, H. M. Goldenberg, and N. F. Ramsey, Phys. Rev. **126**, 603 (1962).
[30]D. Kleppner, H. C. Berg, S. B. Crampton, N. F. Ramsey, R. F. C. Vessot, H. E. Peters, and J. Vanier, Phys. Rev. **138**, A972 (1965).